Protracted treatment with MDMA induces heteromeric nicotinic receptor up-regulation in rat brain: an autoradiography study.

Andrés Ciudad-Roberts, Jorge Camarasa, David Pubill* and Elena Escubedo.

Department of Pharmacology and Therapeutic Chemistry (Pharmacology Section) and Institute of Biomedicine (IBUB), Faculty of Pharmacy, Universitat de Barcelona, Barcelona, Spain.

* Corresponding author:
David Pubill
Department of Pharmacology and Therapeutic Chemistry,
Faculty of Pharmacy,
Universitat de Barcelona,
Av. Joan XXIII s/n
08028 Barcelona, Spain.
Tel: +34-934024531
Fax: +34-934035982
E-mail: d.pubill@ub.edu

Short Title: Regional MDMA-induced nicotinic receptor up-regulation.

Abstract

Previous studies indicate that 3,4-methylenedioxy-methamphetamine (MDMA, ecstasy) can induce heteromeric nicotinic acetylcholine receptor (nAChR, mainly of α4β2 subtype) up-regulation. In this study we treated male Sprague-Dawley rats twice-daily for 10 days with either saline or MDMA (7 mg/kg) and killed them the day after to perform [^{125}I]epibatidine binding autoradiograms on serial coronal slices. MDMA induced significant increases in nAChR density in the substantia nigra, ventral tegmental area, nucleus accumbens, olfactory tubercle, anterior caudate-putamen, somatosensory, motor, auditory and retrosplenial cortex, laterodorsal thalamus nuclei, amygdala, postsubiculum and pontine nuclei. These increases ranged from 3% (retrosplenial cortex) to 30 and 34% (amygdala and substantia nigra). No increased α4 subunit immunoreactivity was found in up-regulated areas compared with saline-treated rats, suggesting a post-translational mechanism as occurs with nicotine. The heteromeric nAChR up-regulation in certain areas could account, at least in part, for the reinforcing, sensitizing and psychiatric disorders observed after long-term consumption of MDMA.

Keywords: MDMA; ecstasy; up-regulation; nicotinic receptor; nicotine; epibatidine

1. Introduction

3,4-Methylenedioxy-methamphetamine (MDMA[1], ecstasy) is a psychostimulant and entactogen amphetamine derivative used illicitly for recreational purposes. Chronic MDMA can induce serotonergic and, to a lesser extent, dopaminergic neurotoxicity in rodents and primates (reviewed by Capela et al., 2009). Such neurotoxicity can be a consequence of coordinated oxidative stress, metabolic compromise and inflammation (reviewed by Yamamoto & Raudensky, 2008) originating upon the interaction of MDMA with several targets such as monoamine transporters. Our research group reported a new target for MDMA involved in its neurotoxicity: the neuronal nicotinic acetylcholine receptors (nAChR). **MDMA behaves as a partial agonist on α7 nAChR, inducing prolonged Ca^{2+} entry, which is related with calpain/caspase 3 activation and citotoxicity (Garcia-Ratés et al., 2010) and as an antagonist on α4β2 nAChR. These effects could attenuate the reported protective effect of a full receptor activation (Mudo et al., 2007). In animal and in *in vitro* models, α7 nAChR antagonists have protective effects against MDMA-induced neurotoxicity and cognitive impairment** (see Pubill et al., 2011 for a review).

nAChR are a family of ligand-gated cation channels widely distributed in the nervous system, whose subunit composition and signalling effects depend on subtype and localization (Albuquerque et al., 2009; Gotti et al., 2007). They exert relevant effects on brain functions, involving fast synaptic transmission, cognitive enhancement, memory or reinforcement, and they are the main target of smoked nicotine. nAChR are pentameric structures formed by the association of α and β subunits and can be either homomeric or heteromeric. Of these combinations, the most abundant are heteromeric $(\alpha4)_2(\beta2)_3$ and homomeric α7 receptors. A particular feature of some nAChR subtypes is that, after chronic nicotine exposure, they undergo radioligand binding up-regulation, changes in stoichiometry and increase in their functional state (functional up-regulation) (reviewed by Gaimarri et al., 2007). Such up-regulation occurs at a post-translational level and several mechanisms have been proposed to explain it, including a chaperone-like maturation enhancing effect of nicotine (Lester et al.,

[1] **Abbreviations**

5-HT, serotonin; DA, dopamine; DAT, dopamine transporter; MDMA, 3,4-methylenedioxy-methamphetamine; nAChR, nicotinic acetylcholine receptor; SERT, serotonin transporter; VTA, ventral tegmental area

2009; Kuryatov et al., 2005; Sallette et al., 2005; Srinivasan et al., 2011) and stabilization of the high-affinity state of the receptors (Vallejo et al., 2005). Moreover, nAChR up-regulation could enhance addiction to nicotine by increasing the pleasant effects of the drug (Govind et al., 2009).

Besides its functional effects, we demonstrated that MDMA also induces *in vitro* up-regulation of both homomeric and heteromeric receptors on PC12 cells (Garcia-Rates et al., 2007), through a mechanism that seemed to mimic that of nicotine. Moreover, in recent *in vivo* studies (Pubill et al., 2013; Ciudad-Roberts et al., 2013), we have demonstrated that the classic neurotoxic treatment schedule of MDMA in rats (20 mg/kg b.i.d, 4 days) induces nAChR up-regulation in gross brain regions thus potentiating the up-regulation induced by nicotine; and that a sensitization schedule of MDMA in mice (5 mg/kg/day for 10 days) leads to heteromeric nAChR up-regulation in cortex. Changes in these receptors could have a role in drug addiction and explain some psychiatric effects of this drug, such as memory impairment and psychoses, among others in which nAChR have been found to play a role (Levin et al., 2002; Martin et al., 2004; Ripoll et al., 2004).

Accordingly this study had two aims: first to assess whether a more protracted MDMA treatment but at a lower dose in rats could induce such up-regulation and, if so, to obtain through radioligand binding autoradiography a more precise mapping of the brain areas and nuclei that undergo this phenomenon.

2. Material and methods

2.1 Drugs and radioligands

Racemic MDMA hydrochloride was obtained from the National Health Laboratory, Barcelona, Spain. Its purity was assessed by spectral analysis. Nicotine bitartrate dihydrate and clomipramine were obtained from Sigma (St. Louis, MO, USA). [^{3}H]epibatidine, [^{3}H]paroxetine and [^{125}I]epibatidine were obtained from Perkin Elmer (Boston, MA, USA). All buffer reagents were of analytical grade and purchased from several commercial sources.

2.2 Animals and treatment

The experimental protocols for the use of animals in this study follow the guidelines set out by the European Communities Council (86/609/EEC) and were supervised by the ethics committee of the University of Barcelona, which specifically approved this study. Efforts were made to minimize suffering and reduce the number of animals used. Male Sprague-Dawley rats weighing 200-230 g (Harlan Ibérica, Barcelona, Spain) were used. They were housed at 21ºC ± 1ºC under a 12 h light/dark cycle with free access to food (standard laboratory diet, Panlab, Barcelona, Spain) and drinking water.

Treatment 1 was conducted in order to determine in several gross brain regions whether the proposed MDMA dosing schedule exerted nAChR up-regulation in a significant manner, using radioligand binding to tissue homogenates and Western blotting of lysates. **10** rats were used for this assay; **5** were administered saline (1 ml/kg) and **5** were administered MDMA (7 mg/kg in 1 ml/kg) subcutaneously twice a day within an interval of 7h. The treatment lasted 10 days and the rats were killed the day after. Given the positive results of this preliminar study, the same treatment was repeated **with 12 more rats (6 saline, 6 MDMA,** treatment 2) **of the same characteristics, following the same dosing schedule** to obtain whole brains in order to perform the autoradiography experiments in slices and undertake a more accurate localization of the areas where up-regulation takes place.

2.3 Tissue processing

The rats were killed by decapitation under isoflurane anaesthesia and the brains were removed rapidly from the skull. In the case of treatment 1, frontal and parietal cortex, striatum, hippocampus, and a coronal slice delimited by the thickness of superior colliculi, after removal of cortex and hippocampus, (from here on out we will refer to this section as "colliculi slice") were quickly excised on a refrigerated surface, frozen on dry ice and stored at –80 °C until later use (Chipana et al., 2008). In the case of treatment 2, whole brains were quickly frozen by short immersion in isopentane pre-cooled in dry ice, then stored at -80°C until slicing for autoradiography experiments.

Samples for use in radioligand binding experiments or Western blot determination were thawed and homogenized in 10 volumes of buffer: 5 mM Tris-HCl, 320 mM sucrose and

protease inhibitors (aprotinin 4.5 µg/µl, 0.1 mM phenylmethylsulfonyl fluoride and 1 mM sodium orthovanadate), pH 7.4, with a Polytron homogenizer. The homogenates were centrifuged at 15,000 x g for 30 min at 4 °C. The resulting pellets were washed twice and the final pellets (crude membrane preparation) were resuspended in 50 mM Tris-HCl buffer. Protein concentration was determined using the BioRad protein reagent (Bio-Rad Labs. Inc., Hercules, CA, USA) according to the manufacturer's instructions and the samples were stored at -80 ºC until later use.

For Western blotting, aliquots of tissue homogenates were centrifuged at 15,000 x g for 30 min at 4ºC. The supernatants were discarded and the pellets were resuspended in an appropriate volume of ice-cold solubilisation buffer consisting of 20 mM Tris HCl pH 8, 137 mM NaCl, 2 mM EDTA, 1% Nonidet P-40, 4.5 µg/µl aprotinin and 0.1 mM phenylmethylsulfonyl fluoride. Proteins were solubilised by incubation for 2 h at 4ºC under gentle rotation. Thereafter, the samples were centrifuged at 15,000 x g for 30 min at 4ºC and the supernatants were stored at -80 ºC after determination of protein content using the Bio-Rad Protein Reagent and bovine serum albumin standards prepared in the same dilution of solubilisation buffer, in order to compensate for the reaction with the buffer detergent.

The samples for use in autoradiography experiments were processed as follows: brains were coronally-sectioned (16 µm thickness) using a Leica CR 3050 S cryostat (chamber temperature: -20 ºC; sample temperature: -16 ºC). Sections were thaw-mounted on Fisher Superfrost Plus microscope slides and immediately returned to the cryostat chamber until storage. Two consecutive sections were mounted on each slide. The slides containing the sections were stored in tightly sealed containers with Drierite bags at –80ºC until use. The sections were numbered according to the most approximate coordinates obtained from the Paxinos & Watson rat brain atlas (2005).

2.4 Radioligand binding assays

[^{3}H]paroxetine binding was used to label serotonin (5-HT) transporters (SERT) in order to assess whether MDMA dosage had caused any serotonergic alterations, including neurotoxic effects (Pubill et al., 2003). Binding was determined in membrane preparations from parietal cortex, an area very sensititive and representative to the effects of MDMA on SERT. Binding was performed in glass tubes containing 0.1 nM [^{3}H]paroxetine and 150 µg of membranes.

Incubation was carried out at 25 ºC for 2 h in a Tris–HCl buffer (50 mM, pH 7.4) containing 120 mM NaCl and 5 mM KCl to a final volume of 1.6 ml. Clomipramine (100 μM) was used to determine non-specific binding.

[^{3}H]epibatidine binding was used to label heteromeric (mainly α4β2) nAChR in order to determine whether MDMA had caused an up-regulation of these receptor types in the gross regions obtained from treatment 1. Concretely, binding was carried out using preparations from rat cortex, striatum and the "colliculi slice". These experiments were performed in glass tubes containing 1 nM [^{3}H]epibatidine and 200 μg of brain membranes. Incubation was carried out at 25 ºC for 2 h in Tris-HCl buffer (50 mM, pH 7.4). Nicotine (300 μM) was used to determine non-specific binding.

Bindings were terminated by rapid vacuum filtration through Whatman GF/B glass fibre filters (Whatman Intl. Ltd., Maidstone, U.K.) presoaked in 0.5% polyethyleneimine. Tubes and filters were washed rapidly 3 times with 4 ml ice-cold 50 mM Tris-HCl. The radioactivity trapped on the filters was measured by liquid scintillation spectrometry. Specific binding was calculated as the difference between the radioactivities measured in the absence (total binding) and in the presence (non-specific binding) of the excess of non-labelled ligand.

2.5 Western blotting and immunodetection

A general Western blotting and immunodetection protocol was used to determine nAChR α4 subunit in the frontal cortex and colliculi slice extracts from treatment 1, which had shown significant [^{3}H]epibatidine binding up-regulation. For each sample, 30 μg of protein was mixed with sample buffer [0.5 M Tris-HCl, pH 6.8, 10% glycerol, 2% (w/v) sodium dodecyl sulphate, 5% (v/v) 2-β-mercaptoethanol, 0.05% bromphenol blue, final concentrations], boiled for 10 min, loaded onto a 10% acrylamide gel and separated by electrophoresis. Proteins were then transferred to polyvinylidene fluoride membranes (Immobilon-P, Millipore, Billerica, MA, USA). Membranes were blocked 1 h at room temperature with 5% bovine serum albumin in Tris-buffered saline buffer plus 0.05% Tween 20 (TBS-T) and incubated overnight at 4ºC with a primary rabbit monoclonal antibody against nAChR α4 subunit (ab124832) purchased from Abcam (Cambridge, UK) and used at a 1:1000 dilution in TBS-T buffer plus 5% bovine serum albumin. After washing, the membranes were incubated with a peroxidase-conjugated anti-rabbit IgG antibody (GE Healthcare, Buckinghamshire,

UK). Immunoreactive protein was visualized using a chemiluminescence-based detection kit (Immobilon Western, Millipore) and a BioRad ChemiDoc XRS gel documentation system. Apparent molecular weight bands corresponding to the target protein was 70 kDa. Scanned blots were analyzed using BioRad Quantity One software. Immunodetection of β-actin (mouse monoclonal anti β-actin antibody, Sigma, St. Louis, USA; dil.1:2500) served as a control of load uniformity for each lane and was used to normalize differences due to protein content. The α4 levels are expressed as a percentage of those obtained from saline-treated animals.

2.6 Autoradiography experiments

Slides containing the brain sections were removed from the -80ºC freezer and left to warm to room temperature. A hydrophobic barrier was drawn around every slice using an ImmEdge™ Pen (Vector Laboratories, Burlingame, CA, USA) to provide a heat-stable, hydrophobic barrier that kept reagents localized on tissue specimens and prevented mixing when multiple sections were mounted on the same slide.

The binding of [^{125}I]epibatidine to brain slices was conducted as follows. After warming, the slides (containing two slices each) were placed on a flat surface and 0.5 ml of binding buffer (50 mM Tris-HCl buffer, pH 7.4; aprotinin 4.5 μg/μl; 0.1 mM phenylmethylsulfonyl fluoride) was distributed onto each sample during 15 min. Thereafter, buffer was aspirated and the samples were pre-incubated again for another 15 min in binding buffer.

In preliminary experiments, one section of each slide was incubated during 1 h in binding buffer containing 0.2 nM [^{125}I]epibatidine and, in order to determine the non-specific binding, the adjacent section was incubated in [^{125}I]epibatidine containing 300 μM nicotine. Under these conditions, non-specific binding in adjacent sections was not distinguishable from background and therefore total binding was identical to specific binding, as previously reported by other groups (Nguyen et al., 2003). Thus further sections were incubated only with [^{125}I]epibatidine to obtain a larger number of sections to quantify. After incubation, the radioligand was aspirated and the samples were washed by immersing each slide in two cubets filled with ice-cold 50 mM Tris-HCl buffer during 5 min each. Samples were finally dipped in ice-cold bidistilled water to remove salts and quickly dried using a stream of cold dry air.

Once slides were completely dry, they were stuck onto a cardboard paper sheet using double-sided tape, together with [^{125}I] standards (American Radiolabeled Chemicals, St. Louis, MO, USA). Slides were then placed into an exposition cassette and covered with a plastic sheet and a phosphor plate (storage phosphor screen GP, Kodak, Rochester, NY, USA) on top of it. Expositions lasted 24-48 h depending on the signal intensity of the areas of interest and plates were scanned at maximum resolution using a phosphorimager (BioRad Personal Molecular Imager, Bio-Rad Labs. Inc., Hercules, CA, USA).

The autoradiography images were processed using BioRad Image Lab software, **where each area or region of interest (ROI) was manually delineated as closely as possible to the actual area delimited by the Paxinos & Watson atlas (2005). The ROI shape was copied/pasted and fitted to the same area of similar slices. Different shapes were made for left and right hemispheres in order to properly adjust to each area.** The corresponding intensity and area values were exported to Microsoft Excel. The mean density count (counts/area) was calculated, the background subtracted and bound radioactivity was determined through 2nd order polynomial (quadratic) interpolation in the curve defined by radioactivity standards using GraphPad Prism 3.0 software. Values were normalized taking into account the radioactivity decay of the radioligand and the standards for each determination day. All the intensity values of the samples fell within the standard curve defined by the radioactivity standards, where the relationship between activity and intensity was practically linear. Data (mean ± SEM) are reported in normalized arbitrary units (AU).

For each rat and brain area, at least 6 values were obtained from different slices **and averaged.** According to the Paxinos and Watson atlas (2005), the caudate-putamen was divided into anterior (plates 13-15) and posterior (plates 16-39) and data represent measurements of the entire area at those levels. Also, thalamic nuclei were grouped into laterodorsal, medial, ventral and ventral pallidum. For visualization purposes, images were converted from grayscale to color spectrum using the Image Lab software.

Note that although a large number of regions (31) were assessed, this was not an exhaustive survey of binding in all brain regions, but a demonstration that MDMA can induce regional nAChR up-regulation.

2.7 Statistical analysis

All data are expressed as mean ± standard error of the mean (S.E.M.) of the values obtained for each treatment group. Unpaired Student's *t*-test for two-sample (saline *vs.* MDMA) was used to analyse the statistical significance ($P<0.05$) of the difference between the means of the two groups. Values of *t*-test and dregrees of freedom (df) are also reported for each comparison.

3. Results

3.1 [^{3}H]Paroxetine binding

There was a significant marked decrease (around 50%) in [^{3}H]paroxetine binding in parietal cortex from the rats treated with MDMA and killed the day after the last dose ($t = 2.88$, df = 8, $P = 0.02$), thus indicating a loss of serotonin transporters (Fig. 1).

3.2 [^{3}H]Epibatidine binding to homogenates

Significant increases ($P<0.05$) in [^{3}H]epibatidine binding were found in the frontal portion of the cortex (24%, $t = 3.42$, df = 7, $P = 0.014$) and the colliculi slice (28%, $t = 5.21$, df = 8, $P = 0.0008$, this slice contains the colliculi, the geniculate nuclei, the substantia nigra (SN) and the ventral tegmental area, (VTA)) originating from MDMA-treated rats (Fig. 2). No significant increases were found in the striatum ($t = 2.023$, df = 8, $P = 0.08$) or in the parietal cortex ($t = 2.24$, df = 7, $P = 0.06$) although a tendency towards increase can be observed.

3.3 Western blot of α4 protein

In order to determine whether the increase in α4β2 nAChR observed in treatment 1 was due to increased protein synthesis or to post-translational modifications, α4 subunits were immunodetected in the lysates from the areas where significant increases in [^{3}H]epibatidine binding were found, namely the frontal cortex and the colliculi slice . No significant changes were observed between the subunit levels of saline and MDMA-treated rats (Fig. 3) (frontal cortex: $t = 0.59$, df = 8, $P = 0.57$; colliculi slice: $t = 0.25$, df =8, $P = 0.80$).

3.4 [^{125}I]Epibatidine autoradiography

[^{125}I]Epibatidine labelled heteromeric nAChR in accordance with the established patterns in previous publications (i.e. Nguyen et al., 2003; Tribollet et al., 2004). Intermediate nAChR levels were found in cortex, striatum, thalamic nuclei, geniculate nuclei and SN. Receptor density was most intense in the superior colliculi, medial habenula and interpeduncular nucleus, while hippocampus and hypothalamus showed the lowest nAChR levels.

MDMA-treated animals showed a significant increase in nAChR density in the SN, VTA, nucleus accumbens, olfactory tubercle, anterior caudate-putamen, somatosensory, motor, auditory, and retrosplenial cortex, laterodorsal thalamuic nuclei, amygdala, postsubiculum and pontine nuclei (Table I). These increases (Table 1 and Fig. 4) ranged from 3% (retrosplenial cortex) to 30 and 34% (amygdala and SN). The rest of areas showed no significant difference between saline and MDMA-treated rats.

Discussion

In this study we have demonstrated, using the radioligand autoradiography technique, that a prolonged treatment with the psychostimulant drug MDMA induces up-regulation of heteromeric nAChR (which in the brain are mainly α4β2) in specific areas of the rat brain. This is in agreement with our previous reports showing this effect in cultured PC 12 cells (Garcia-Ratés et al., 2007), in gross brain areas after the classical neurotoxic schedule (Pubill et al., 2013) or in mice after a sensitizing schedule (Ciudad-Roberts et al., 2013). MDMA has affinity for α4β2 nAChR (Garcia-Ratés et al., 2007; Chipana et al., 2008) as occurs with several nicotinic ligands, either agonists or antagonists, that have been reported to induce nAChR up-regulation (Peng et al., 1994; Gopalakrishnan et al., 1997).

Binding to homogenates from gross brain areas is useful for screening purposes, but is not accurate enough to ascertain the changes in small areas that are involved in specific brain functions. Also, if the increase took place only in a small area that is part of a gross portion used for the assay, this increase would not be detected owing to the dilution effect (as we found, for example, in the different parts of the striatum). Thus, looking at the previous results, it was mandatory to carry out an autoradiography study in brain slices to determine nAChR levels in more defined areas.

In addition, we used lower MDMA doses than in the previous study (Pubill et al., 2012), during an extended treatment period at normal housing temperature in order to reduce serotonergic neurotoxicity that could hinder nAChR up-regulation (Gordon et al., 1991; Green et al., 2005). In this respect we must point out that regardless of the conditions of this treatment, we found a marked loss of paroxetine binding sites, which has been generally linked to serotonergic neurotoxicity. However, we must point out that in our treatment the rats were killed 24 h after the last dose, while most studies (i.e. Biezonski & Meyer, 2010; Broening et al., 1995; Malberg et al., 1998; O'Shea et al., 1998) make the measurement after leaving a time of at least one week to allow the neurotoxic process to occur. We cannot assert whether the decrease in paroxetine binding is due to serotonergic terminal degeneration or to a regulatory process. In fact, a significant reduction in SERT gene expression, which could explain a reduction in SERT protein irrespective of altered terminal integrity, has been reported after treatment with MDMA (Biezonski & Meyer, 2010). As will be discussed below, as a number of presynaptic nAChR are localized on serotonergic terminals and **there seems to be** a positive correlation between their up-regulation and SERT, it can be suggested that the decrease in paroxetine binding in this study is most likely to be due to a regulatory process rather than to terminal destruction.

As most up-regulation studies carrried out with nicotine use continuous dosing through prolonged constant infusion or osmotic minipumps (i.e. Nguyen et al., 2003) we chose a MDMA dosing schedule aimed to reach sufficient plasma levels during enough time to induce up-regulation with reduced neurotoxic potential, compared with our previous work in gross brain areas. This schedule, therefore, was not intended to model any human consumption pattern but to demonstrate and localize nAChR up-regulation by MDMA. Once this was demonstrated, further work using other schedules closer to recreational use patterns should be performed.

Phosphor imaging was used in order to obtain and quantify the images. Traditionally, *in situ* autoradiography has been performed using X-ray film, which provides the highest resolution. However, depending on the radioligand used, exposure times with films are much longer than those with phosphor plates and, due to the evolution and raise of the digital imaging systems, obtaining suitable and affordable X-ray films is becoming more and more difficult. As an alternative, quantitative phosphor imaging provides lower exposure time, economization due to the reutilization of phosphor screens, no waste of developing solutions, direct quantification on the scanned digital image and an optical resolution suitable for most

quantitative purposes (Strome et al., 2005). This technique was used by another group for quantifying α7 nAChR using [^{3}H]methyllycaconitine (Mugnaini et al., 2002) and, to our knowledge, the present study is the first employing this technique to quantify heteromeric nAChR using [^{125}I]epibatidine.

A number of studies carried out with nicotine have suggested several mechanisms to explain nAChR up-regulation (see Introduction), and most agree on the fact that up-regulation occurs at a post-translational level. To assess this possibility with MDMA we analyzed by Western blot the α4 subunit levels in the same protein samples from brain portions that had showed increased epibatidine binding in homogenates and compared them with those from saline-treated rats. No significant differences were found between the two groups, indicating that up-regulation of binding takes place without increased protein levels, probably through post-translational modifications that increase the affinity or promote maturation of receptors towards a form capable of binding the ligand, similarly to what has been described for nicotine in the articles referenced above.

nAChR have a predominant presynaptic localization, on the nerve endings, where they modulate the release of key neurotransmitters such as acetylcholine, dopamine (DA), GABA, glutamate and serotonin (reviewed by Marchi & Grilli, 2010), although they are also at the preterminal level and on different postsynaptic locations in the brain (Mameli-Engvall et al., 2006). NAChR play a key role in addiction to nicotine (Govind et al., 2009). It has been described that the addictive effects of nicotine are produced through its interaction with nAChR in the mesolimbic pathway, especially those in the nucleus accumbens, leading to DA release that activates the reward circuitry. In fact, mice with deletion of the β2 gene do not self-administer nicotine after previous administration and do not show increased release of DA in the ventral tegmental area (Picciotto et al., 1999).

Although the mechanisms involved in the establishment of addiction are complex and still being investigated, up-regulation of nAChR increasing the pleasant effects of the drug is an event that could feasibly play a role. In the present study, we demonstrate nAChR up-regulation in key areas involved in addiction, such as the VTA, the nucleus accumbens and several areas of the cortex that are involved in sensory and motor functions (i.e. auditory, somatosensory, motor), as well as in the olfactory tubercle. Heteromeric nAChR play a role in the hyperlocomotion induced by amphetamine derivatives (Camarasa et al., 2009; Ciudad-

Roberts et al., 2013), thus an increase in nAChR in these areas could account for sensitization to the locomotor effects and the addictive properties of MDMA. In fact, blockade of nAChR containing the α4 subunit with dihydro-β-erythroidine or varenicline inhibits the hyperlocomotion induced by MDMA in mice, as well as an increased delayed sensitization (Ciudad-Roberts et al., 2013). Moreover, in the same study it was demonstrated that pretreatment with nicotine inducing nAChR up-regulation reduced the dose threshold for MDMA-conditioned place preference.

In the olfactory tubercle, an area that underwent a 20% increase, β2 subunit-containing nAChR increase DA release (Grady et al., 2002). This area is a component of the ventral striatum, it is heavily interconnected with several affective, reward and motivation related centers of the brain, being the area that modulates behaviour during certain physiological and mental states (Weeson & Wilson, 2011). The olfactory tubercle has also been shown to be especially involved in reward and addictive behaviours, so that rats have been shown to self-administer cocaine into this area more than the nucleus accumbens and ventral pallidum (Ikemoto, 2003). Also, the olfactory tubercle receives an important serotonergic innervation (Cumming et al., 1997). Therefore the up-regulation found in this area could also account for reinforcing effects after a chronic treatment.

The nigrostriatal pathway was also affected by nAChR up-regulation, as we found a 33% increase in subtantia nigra as well as a 16% increase in the anterior caudate-putamen. α4β2 nAChR have been identified in soma and dendrites of SN, as well as in the dopaminergic terminals in the striatum (Jones et al., 2001). Dopaminergic neurones from the SN possess the ability to release DA not only from axon terminals in striatum, but also from the soma and dendrites within SN (Cheramy et al., 1981). It has been suggested that serotonergic afferents to SN may evoke this dendritic dopamine release through a mechanism that is uncoupled from the impulse-dependent control of nerve terminal DA release (Cobb & Abercrombie, 2003).

Nicotine and nicotinic agonists increase DA release from mesolimbic and nigrostriatal neurones *in vitro* and *in vivo* (Wonnacott, 1997). In the striatum, an important percentage of β2 subunit-containing nAChR is associated to dopaminergic buttons from the nigrostriatal pathway, and the rest may correspond to other neurotransmitter afferents such as serotonergic fibers coming from the dorsal raphe nucleus (Jones et al., 2001; Reuben & Clarke, 2000;

Schwartz et al., 1984). As this pathway is involved in the control of movement, increased nAChR in the striatal DA terminals could be involved in motor disorders or stereotypies.

Previous studies on nicotine-induced nAChR up-regulation indicate that chronic nicotine exposure differentially affects the number (up-regulation), subunit composition, stochiometry and functional status of some nAChR subtypes, leaving others substantially unaffected (Gaimarri et al., 2007). In this respect, when comparing the results of the present study with those obtained from chronic nicotine-treated rats by Nguyen et al. (2003) in the same brain areas, we can find similarities regarding these aspects. For example, in both studies, the amygdala and the substantia nigra exhibit some of the highest up-regulation rates, while other areas with a high density of nAChR such as the interpeduncular nucleus or the medial habenula show no change in radioligand binding. The nucleus accumbens undergoes the highest up-regulation in the corpus striatum, while in the caudate-putamen it is more modest. Conversely, some areas within the cortex and the hippocampus that had shown robust nAChR up-regulation after nicotine administration were unaffected or showed a lower effect in our study. We have cited above that nAChR up-regulation by nicotine and MDMA is a mechanistically-complex process that implies the interaction of the ligand with intracellular immature forms of the receptor. Nicotine is known to penetrate the cell membrane (Whiteaker et al., 1998), which allows such an interaction to occur, while MDMA is known to use the monoamine transporters, mainly the SERT (Fitzgerald et al., 1990), to access the intracellular compartments. Thus the different ability of each brain area to take up MDMA could explain the main differences found in comparison to nicotine.

Moreover, when looking at previous literature such as the article from Battaglia et al. (1991), who similarly quantified the levels of SERT in brains from rats of the same strain, gender and age than ours, we found that the areas with increased epibatidine binding tend to correspond with areas having higher SERT levels in control animals. In fact, it has been reported that a single acute *in vivo* exposure to nicotine significantly increases 5-HT uptake via SERT in prefrontocortical synaptosomes (Awtry & Werling, 2003), which indicates that there is a regulatory interaction between nAChR and SERT. In this respect we noticed that SERT density in the areas showing greatest nAChR up-regulation by MDMA was not affected (amygdala and VTA) or even increased (substantia nigra, nucleus accumbens) by MDMA in the study from Battaglia et al. (1991). On the other hand, areas from the cortex and hippocampus which are capable of showing a robust nAChR up-

regulation by nicotine, suffer from a strong reduction of SERT after MDMA, as we also assessed in cortex homogenate in the present study; this could explain why these areas show a lower radioligand binding increase after treatment with this amphetamine derivative, as this would difficult its internalization in the synaptic terminal, thus impeding nAChR up-regulation. **Nonetheless, further investigation should be conducted to pursue this hypothesis.**

The predominantly presynaptic localization and widespread distribution of nAChR in several brain circuits makes it particularly difficult to functionally characterize the specific behavioral or brain roles affected by MDMA-induced up-regulation; nonetheless the present results can illustrate which functions could probably be altered and suggest a mechanism to explain, at least in part, the reinforcing properties of MDMA.

Conclusion

In this study we demonstrate that a protracted treatment with MDMA induces heteromeric nAChR up-regulation in key areas of rat brain involved in motivation and learning, sensory and movement control, which could account for reinforcing and some neuropsychiatric disorders related with chronic consumption of this drug.

Translated to a clinical context, we show nAChR as a potential target for reducing MDMA's reinforcing effects. Furthermore, we also postulate that nAChR up-regulation induced by chronic consumption of MDMA could potentiate the ability of other drugs to cause addiction due to an enhancement of nAChR-mediated reinforcing effects.

Disclosure Statement

All authors declare no actual or potential conflict of interest including financial, personal or other relationships with other people or organizations that could inappropriately influence the present work. All authors reviewed the content and approved the final version.

Contributors

DP and EE were responsible for the study concept and design. AC and DP performed the experiments. EE and JC contributed to animal treatment. DP and JC performed data analysis. DP wrote the manuscript draft and AC revised language. JC and EE interpreted findings and provided critical revision of the manuscript.

Acknowledgements

The authors wish to acknowledge A. Ciudad-Roberts for language revisions on the manuscript and Alba Albertí for technical assistance. This study was supported by the following grants from: the regional authorities Generalitat de Catalunya (2009SGR 977) to DP; the Spanish drug initiative Plan Nacional sobre Drogas (2008I003) to DP and the Spanish Ministerio de Ciencia e Innovación (SAF2010-15948) to EE. The funding sources had no involvement in writing, providing advice on or submitting this report.

References

Albuquerque, E.X., Pereira, E.F., Alkondon, M., Rogers, S.W., 2009. Mammalian nicotinic acetylcholine receptors: from structure to function. Physiol. Rev. 89, 73-120.

Awtry, T.L., Werling, L.L., 2003. Acute and chronic effects of nicotine on serotonin uptake in prefrontal cortex and hippocampus of rats. Synapse 50, 206-211.

Battaglia, G., Sharkey, J., Kuhar, M.J., de Souza, E.B., 1991. Neuroanatomic specificity and time course of alterations in rat brain serotonergic pathways induced by MDMA (3,4-methylenedioxymethamphetamine): assessment using quantitative autoradiography. Synapse 8, 249-260.

Biezonski, D.K., Meyer, J.S., 2010. Effects of 3,4-methylenedioxymethamphetamine (MDMA) on serotonin transporter and vesicular monoamine transporter 2 protein and gene expression in rats: implications for MDMA neurotoxicity. J. Neurochem. 112, 951-962.

Broening, H.W., Bowyer, J.F., Slikker, W., 1995. Age-dependent sensitivity of rats to the long-term effects of the serotonergic neurotoxicant (+/-)-3,4-methylenedioxymethamphetamine (MDMA) correlates with the magnitude of the MDMA-induced thermal response. J. Pharmacol. Exp. Ther. 275, 325-333.

Camarasa, J., Garcia-Rates, S., Pubill, D., Escubedo, E., 2009. The involvement of nicotinic receptor subtypes in the locomotor activity and analgesia induced by methamphetamine in mice. Behav. Pharmacol. 20, 623-630.

Capela, J.P., Carmo, H., Remiao, F., Bastos, M.L., Meisel, A., Carvalho, F., 2009. Molecular and cellular mechanisms of ecstasy-induced neurotoxicity: an overview. Mol. Neurobiol. 39, 210-271.

Cheramy, A., Leviel, V., Glowinski, J., 1981. Dendritic release of dopamine in the substantia nigra. Nature 289, 537-542.

Chipana, C., Garcia-Rates, S., Camarasa, J., Pubill, D., Escubedo, E., 2008. Different oxidative profile and nicotinic receptor interaction of amphetamine and 3,4-methylenedioxy-methamphetamine. Neurochem. Int. 52, 401-410.

Ciudad-Roberts, A., Camarasa, J., Pubill, D. Escubedo, E., 2013. Heteromeric nicotinic receptors are involved in the sensitization and addictive properties of MDMA in mice. Prog. Neuropsychopharmacol. Biol. Psychiatry. 44, 201-209
.
Cobb, W.S., Abercrombie, E.D., 2003. Relative involvement of globus pallidus and subthalamic nucleus in the regulation of somatodendritic dopamine release in substantia nigra is dopamine-dependent. Neuroscience 119, 777-786.

Cumming, P., Ljubic-Thibal, V., Laliberte, C., Diksic, M., 1997. The effect of unilateral neurotoxic lesions to serotonin fibres in the medial forebrain bundle on the metabolism of [3H]DOPA in the telencephalon of the living rat. Brain Res. 747, 60-69.

Fitzgerald,J.L., Reid,J.J., 1990. Effects of methylenedioxymethamphetamine on the release of monoamines from rat brain slices. Eur. J. Pharmacol. 191, 217-220.

Gaimarri, A., Moretti, M., Riganti, L., Zanardi, A., Clementi, F., Gotti, C., 2007. Regulation of neuronal nicotinic receptor traffic and expression. Brain Res. Rev. 55, 134-143.

Garcia-Rates, S., Camarasa, J., Escubedo, E., Pubill, D., 2007. Methamphetamine and 3,4-methylenedioxymethamphetamine interact with central nicotinic receptors and induce their up-regulation. Toxicol. Appl. Pharmacol 223, 195-205.

Garcia-Rates, S., Camarasa, J., Sanchez-Garcia, A. I., Gandia, L., Escubedo, E., Pubill, D., 2010. The effects of 3,4-methylenedioxymethamphetamine (MDMA) on nicotinic receptors: intracellular calcium increase, calpain/caspase 3 activation, and functional upregulation. Toxicol. Appl. Pharmacol. 244, 344-353.

Gopalakrishnan, M., Molinari, E.J., Sullivan, J.P., 1997. Regulation of human alpha4beta2 neuronal nicotinic acetylcholine receptors by cholinergic channel ligands and second messenger pathways. Mol. Pharmacol. 52, 524-534.

Gordon, C.J., Watkinson, W.P., O'Callaghan, J.P., Miller, D.B., 1991. Effects of 3,4-methylenedioxymethamphetamine on autonomic thermoregulatory responses of the rat. Pharmacol. Biochem. Behav. 38, 339-344.

Gotti, C., Moretti, M., Gaimarri, A., Zanardi, A., Clementi, F., Zoli, M., 2007. Heterogeneity and complexity of native brain nicotinic receptors. Biochem. Pharmacol. 74, 1102-1111.

Govind, A.P., Vezina, P., Green, W.N., 2009. Nicotine-induced upregulation of nicotinic receptors: underlying mechanisms and relevance to nicotine addiction. Biochem.Pharmacol. 78, 756-765.

Grady, S.R., Murphy, K.L., Cao, J., Marks, M.J., McIntosh,J .M., Collins, A.C., 2002. Characterization of nicotinic agonist-induced [3H]dopamine release from synaptosomes prepared from four mouse brain regions. J. Pharmacol. Exp. Ther. 301, 651-660.

Green, A.R., O'Shea, E., Saadat, K.S., Elliott, J.M., Colado, M.I., 2005. Studies on the effect of MDMA ('ecstasy') on the body temperature of rats housed at different ambient room temperatures. Br. J. Pharmacol. 146, 306-312.

Ikemoto, S., 2003. Involvement of the olfactory tubercle in cocaine reward: intracranial self-administration studies. J. Neurosci. 23, 9305-9311.

Jones, I.W., Bolam, J.P., Wonnacott, S., 2001. Presynaptic localisation of the nicotinic acetylcholine receptor beta2 subunit immunoreactivity in rat nigrostriatal dopaminergic neurones. J. Comp. Neurol. 439, 235-247.

Kuryatov, A., Luo, J., Cooper, J., Lindstrom, J., 2005. Nicotine acts as a pharmacological chaperone to up-regulate human alpha4beta2 acetylcholine receptors. Mol. Pharmacol. 68, 1839-1851.

Lester, H.A., Xiao, C., Srinivasan, R., Son, C.D., Miwa, J., Pantoja, R., Banghart, M.R., Dougherty, D.A., Goate, A.M., Wang, J.C., 2009. Nicotine is a selective pharmacological chaperone of acetylcholine receptor number and stoichiometry. Implications for drug discovery. AAPS J. 11, 167-177.

Levin, E.D., Rezvani, A.H., 2002. Nicotinic treatment for cognitive dysfunction. Curr. Drug Targets. CNS Neurol. Disord. 1, 423-431.

Malberg, J.E., Seiden, L.S., 1998. Small changes in ambient temperature cause large changes in 3,4-methylenedioxymethamphetamine (MDMA)-induced serotonin neurotoxicity and core body temperature in the rat. J. Neurosci. 18, 5086-5094.

Mameli-Engvall, M., Evrard, A., Pons, S., Maskos, U., Svensson, T.H., Changeux, J.P., Faure, P., 2006. Hierarchical control of dopamine neuron-firing patterns by nicotinic receptors. Neuron 50, 911-921.

Marchi, M., Grilli, M., 2010. Presynaptic nicotinic receptors modulating neurotransmitter release in the central nervous system: functional interactions with other coexisting receptors. Prog. Neurobiol. 92, 105-111.

Martin, L.F., Kem, W.R., Freedman, R., 2004. Alpha-7 nicotinic receptor agonists: potential new candidates for the treatment of schizophrenia. Psychopharmacology (Berl) 174, 54-64.

Mudo, G., Belluardo, N., Fuxe, K., 2007. Nicotinic receptor agonists as neuroprotective/neurotrophic drugs. Progress in molecular mechanisms. J. Neural Transm. 114, 135-147.

Mugnaini, M., Tessari, M., Tarter, G., Merlo, P.E., Chiamulera, C., Bunnemann, B., 2002. Upregulation of [3H]methyllycaconitine binding sites following continuous infusion of

nicotine, without changes of alpha7 or alpha6 subunit mRNA: an autoradiography and in situ hybridization study in rat brain. Eur. J. Neurosci. 16, 1633-1646.

Nguyen, H.N., Rasmussen, B.A., Perry, D.C., 2003. Subtype-selective up-regulation by chronic nicotine of high-affinity nicotinic receptors in rat brain demonstrated by receptor autoradiography. J. Pharmacol. Exp. Ther. 307, 1090-1097.

O'Shea, E., Granados, R., Esteban, B., Colado, M.I., Green, A.R., 1998. The relationship between the degree of neurodegeneration of rat brain 5-HT nerve terminals and the dose and frequency of administration of MDMA ('ecstasy'). Neuropharmacology 37, 919-926.

Paxinos, G., Watson, C., 2005. The Rat Brain in Stereotaxic Coordinates. Elsevier Academic Press. Amsterdam

Peng, X., Gerzanich, V., Anand, R., Whiting, P.J., Lindstrom, J., 1994. Nicotine-induced increase in neuronal nicotinic receptors results from a decrease in the rate of receptor turnover. Mol. Pharmacol. 46, 523-530.

Picciotto, M.R., Zoli, M., Changeux, J.P., 1999. Use of knock-out mice to determine the molecular basis for the actions of nicotine. Nicotine Tob. Res. 1 Suppl 2, S121-S125.

Pubill, D., Canudas, A.M., Pallas, M., Camins, A., Camarasa, J., Escubedo, E., 2003. Different glial response to methamphetamine- and methylenedioxymethamphetamine-induced neurotoxicity. Naunyn Schmiedebergs Arch. Pharmacol. 367, 490-499.

Pubill, D., Garcia-Rates, S., Camarasa, J., Escubedo, E. 2011. Neuronal nicotinic receptors as new targets for amphetamine-induced oxidative damage and neurotoxicity. Pharmaceuticals 4, 822-847.

Pubill, D., Garcia-Rates, S., Camarasa, J., Escubedo, E., 2012. 3,4-Methylenedioxy-methamphetamine induces in vivo regional up-regulation of central nicotinic receptors in rats and potentiates the regulatory effects of nicotine on these receptors. Neurotoxicology 35C, 41-49.

Reuben, M., Clarke, P.B., 2000. Nicotine-evoked [3H]5-hydroxytryptamine release from rat striatal synaptosomes. Neuropharmacology 39, 290-299.

Ripoll, N., Bronnec, M., Bourin, M., 2004. Nicotinic receptors and schizophrenia. Curr. Med. Res. Opin. 20, 1057-1074.

Sallette, J., Pons, S., Devillers-Thiery, A., Soudant, M., Prado, D.C., Changeux,J.P., Corringer, P.J., 2005. Nicotine upregulates its own receptors through enhanced intracellular maturation. Neuron 46, 595-607.

Schwartz, R.D., Lehmann, J. & Kellar, K.J., (1984) Presynaptic nicotinic cholinergic receptors labeled by [3H]acetylcholine on catecholamine and serotonin axons in brain. J. Neurochem. 42, 1495-1498.

Srinivasan, R., Pantoja, R., Moss, F.J., Mackey, E.D., Son, C.D., Miwa, J., Lester, H.A., 2011. Nicotine up-regulates alpha4beta2 nicotinic receptors and ER exit sites via stoichiometry-dependent chaperoning. J. Gen. Physiol. 137, 59-79.

Strome, E.M., Jivan, S., Doudet, D.J., 2005. Quantitative in vitro phosphor imaging using [3H] and [18F] radioligands: the effects of chronic desipramine treatment on serotonin 5-HT2 receptors. J. Neurosci. Methods 141, 143-154.

Tribollet, E., Bertrand, D., Marguerat, A., Raggenbass, M., 2004. Comparative distribution of nicotinic receptor subtypes during development, adulthood and aging: an autoradiographic study in the rat brain. Neuroscience 124, 405-420.

Vallejo, Y.F., Buisson, B., Bertrand, D., Green, W.N., 2005. Chronic nicotine exposure upregulates nicotinic receptors by a novel mechanism. J. Neurosci. 25, 5563-5572.

Wesson, D.W., Wilson, D.A., 2011. Sniffing out the contributions of the olfactory tubercle to the sense of smell: hedonics, sensory integration, and more? Neurosci. Biobehav. Rev. 35, 655-668.

Whiteaker,P., Sharples,C.G., Wonnacott,S., 1998. Agonist-induced up-regulation of alpha4beta2 nicotinic acetylcholine receptors in M10 cells: pharmacological and spatial definition. Mol. Pharmacol. 53, 950-962.

Wonnacott, S., 1997. Presynaptic nicotinic ACh receptors. Trends Neurosci. 20, 92-98.

Yamamoto, B.K., Raudensky, J., 2008. The role of oxidative stress, metabolic compromise, and inflammation in neuronal injury produced by amphetamine-related drugs of abuse. J. Neuroimmune. Pharmacol. 3, 203-217.

Table 1. [^{125}I]Epibatidine binding to several brain areas of saline- and MDMA-treated rats.

Area	Saline	MDMA	t, df	P	Increase (%)
Frontal cortex	23.53 ± 0.98	23.69 ± 0.65	0.123, 9	n.s.	
Anterior olfactory nucleus	15.45 ± 1.03	14.64 ± 0.92	0.586, 8	n.s.	
Nucleus accumbens	23.69 ± 0.84	27.79 ± 1.19	2.815, 10	<0.05	17
Cingulate cortex	24.85 ± 0.78	25.88 ± 0.72	0.970, 10	n.s.	
Motor cortex	21.07 ± 0.32	23.07 ± 0.80	2.321, 8	<0.05	10
Somatosensory cortex	26.25 ± 0.44	28.86 ± 0.93	2.368, 9	<0.05	10
Insular cortex	16.57 ± 1.44	16.85 ± 0.93	0.163, 10	n.s.	
Olfactory tubercle	18.81 ± 0.89	22.62 ± 0.34	3.697, 9	<0.01	20
Retrosplenial cortex	31.10 ± 0.26	32.14 ± 0.27	2.739, 9	<0.05	3
Visual cortex	23.22 ± 0.60	24.83 ± 2.06	0.750, 10	n.s.	
Auditory cortex	25.79 ± 0.49	28.76 ± 1.06	2.371, 9	<0.05	12
Caudate-putamen					
anterior	31.91 ± 1.73	37.03 ± 1.68	2.253, 10	<0.05	16
posterior	21.62 ± 2.44	21.77 ± 0.72	0.059, 10	n.s.	
Hippocampus (CA1)	13.94 ± 0.68	14.92 ± 0.57	1.104, 10	n.s.	
Hippocampus (dentate gyrus)	19.32 ± 2.58	18.98 ±1.42	0.115, 10	n.s.	
Medial habenula	83.57 ± 3.21	79.79 ± 3.73	0.768, 8	n.s.	
Ventral pallidum	57.99 ± 1.35	58.08 ± 1.46	0.045, 10	n.s.	
Laterodorsal thalamic nuclei	69.68 ± 1.93	77.33 ± 1.77	2.921, 10	<0.01	11
Ventral thalamic nuclei	66.08 ± 1.62	65.38 ± 0.62	0.403, 10	n.s.	
Medial thalamic nuclei	60.69 ± 1.41	61.08 ± 1.86	0.167, 10	n.s.	
Hypothalamus	23.22 ± 0.60	24.83 ± 2.06	0.815, 9	n.s.	
Amygdala	15.78 ± 1.27	20.48 ± 0.89	3.031, 10	<0.05	30
Dorsal lateral geniculate nuclei	57.96 ± 6.45	49.49 ± 3.09	1.184, 8	n.s.	
Superior colliculus, superficial gray layer	49.97 ± 4.12	52.13 ± 1.52	0.492, 8	n.s.	
Medial geniculate nuclei	35.3 ± 4.65	38.97 ± 1.09	0.768, 8	n.s.	
Substantia nigra	27.52 ± 3.59	36.81 ± 0.96	2.287, 9	<0.05	34
Ventral tegmental area	27.47 ± 1.69	33.15 ± 0.69	3.112, 10	<0.05	21
Pontine nuclei	19.37 ± 0.39	22.72 ± 1.12	2.825, 8	<0.05	17
Interpeduncular nucleus	81.51 ± 2.92	91.41 ± 4.78	1.767, 8	n.s.	
Postsubiculum	46.33 ± 1.8	52.4 ± 1.24	2.777, 8	<0.05	13
Cerebellum	10.45 ± 0.52	10.20 ± 0.49	0.350, 8	n.s.	

Semi-quantitative analysis of [^{125}I]epibatidine binding to several areas of brain slices from rats treated with saline (Ctrl) or MDMA (7 mg/kg/day, b.i.d, 10 days). Data (mean ± SEM from 5-6 animals per group) are reported in normalized arbitrary units. P indicates the degree of statistical significance; n.s., non significant (P>0.05); t is Student's t value and df is the degrees of freedom.

Figure captions

Figure 1.

Levels of serotonin transporters (SERT), measured as [^{3}H]paroxetine binding, in membranes from parietal cortex of saline- and MDMA-treated rats. Male Sprague-Dawley rats were treated for 10 days b.i.d. with a dose of MDMA (7 mg/kg) or saline and were sacrificed the day after after. Results are shown as mean ± SEM of the values from 6 animals per group. **P<0.01 *vs.* saline group.

Figure 2.

Density of heteromeric nAChR, measured as [^{3}H]epibatidine binding, in membranes from gross areas of brains from saline- and MDMA-treated rats. Rats were treated for 10 days b.i.d. with a dose of MDMA (7 mg/kg) or saline and were sacrificed on day 11. Binding was assessed in frontal cortex (Fr-CTX), parietal cortex (Par-CTX), the coronal slice of mesencephalon defined by the thickness of superior colliculi (Col. slc) and the striatum (ST). Results are shown as mean ± SEM of the values from 6 animals per group. * P<0.05 and ***P<0.001 *vs.* the same area of saline group.

Figure 3.

Western blot analysis of α4 nAChR subunit in protein extracts of the colliculi slice (Col. slc) and frontal cortex (Fr-CTX) from rats treated for 10 days b.i.d. with a dose of MDMA (7 mg/kg) or saline and sacrificed the day after. Bar graph (panel A) shows overall quantification expressed as percentage over control (6 animals per group, mean ± SEM), while a representative autoradiography from each area (panels B and C) is shown below. β-actin levels were used to ensure gel-loading uniformity and normalize the protein values accordingly.

Figure 4.

Representative images of [^{125}I]epibatidine binding to brain slices from rats treated for 10 days b.i.d. with saline or MDMA (7 mg/kg) and sacrificed the day after. All the labelled regions are illustrated. Numbers on the bottom left corner of photographs indicate the approximate distance of the sections from the coronal plane passing through bregma according to Paxinos and Watson (2005). Panel A shows the grayscale scanned images, while panel B shows the

same images converted to colour spectrum which allows improved visual appreciation of the receptor densities. Abbreviations used (in order of appearance): Fr, frontal cortex; AO, anterior olfactory nucleus; Acb, nucleus accumbens; Cg, gingulate cortex; M, motor cortex; S, somatosensory cortex; I, insular cortex; OT, olfactory tubercle; RS, retrosplenial cortex; V, visual cortex; Au, auditory cortex; HC, hippocampus; MHb, medial habenula; VP, ventral pallidum; LD, laterodorsal thalamic nuclei; VThn, ventral thalamic nuclei; MThn, medial thalamic nuclei; HT, hypothalamus; Amy, amygdala; DLG, dorsal lateral thalamic nuclei; SuG, superior colliculus, superficial gray layer; MG, medial geniculate nuclei; SN, substantia nigra; VTA, ventral tegmental area; PN, pontine nuclei, IP, interpeduncular nucleus; P, postsubiculum, CB, cerebellum.

Figure 1

Click here to download high resolution image

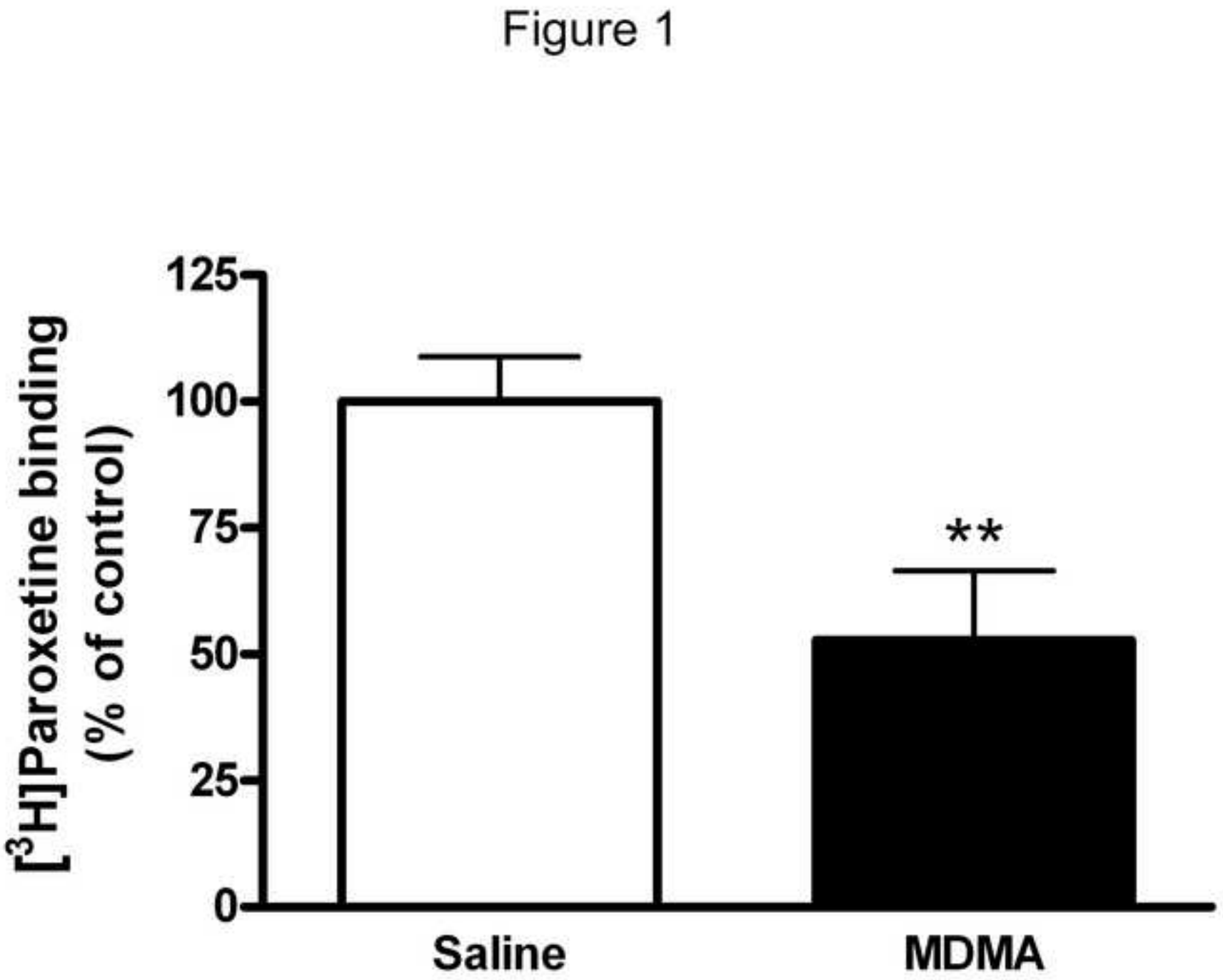

Figure 2

Click here to download high resolution image

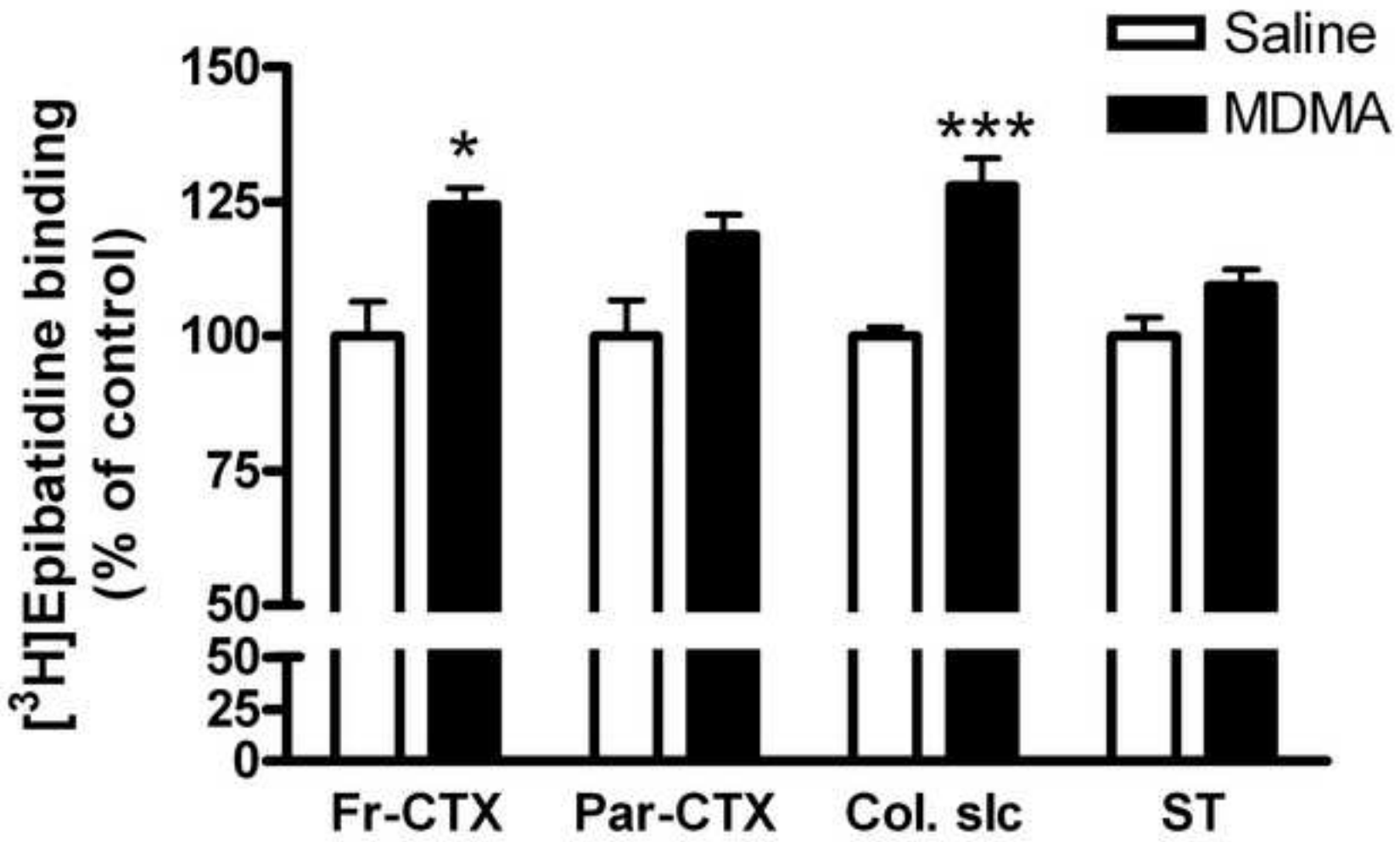

Figure 3
Click here to download high resolution image

Figure 3

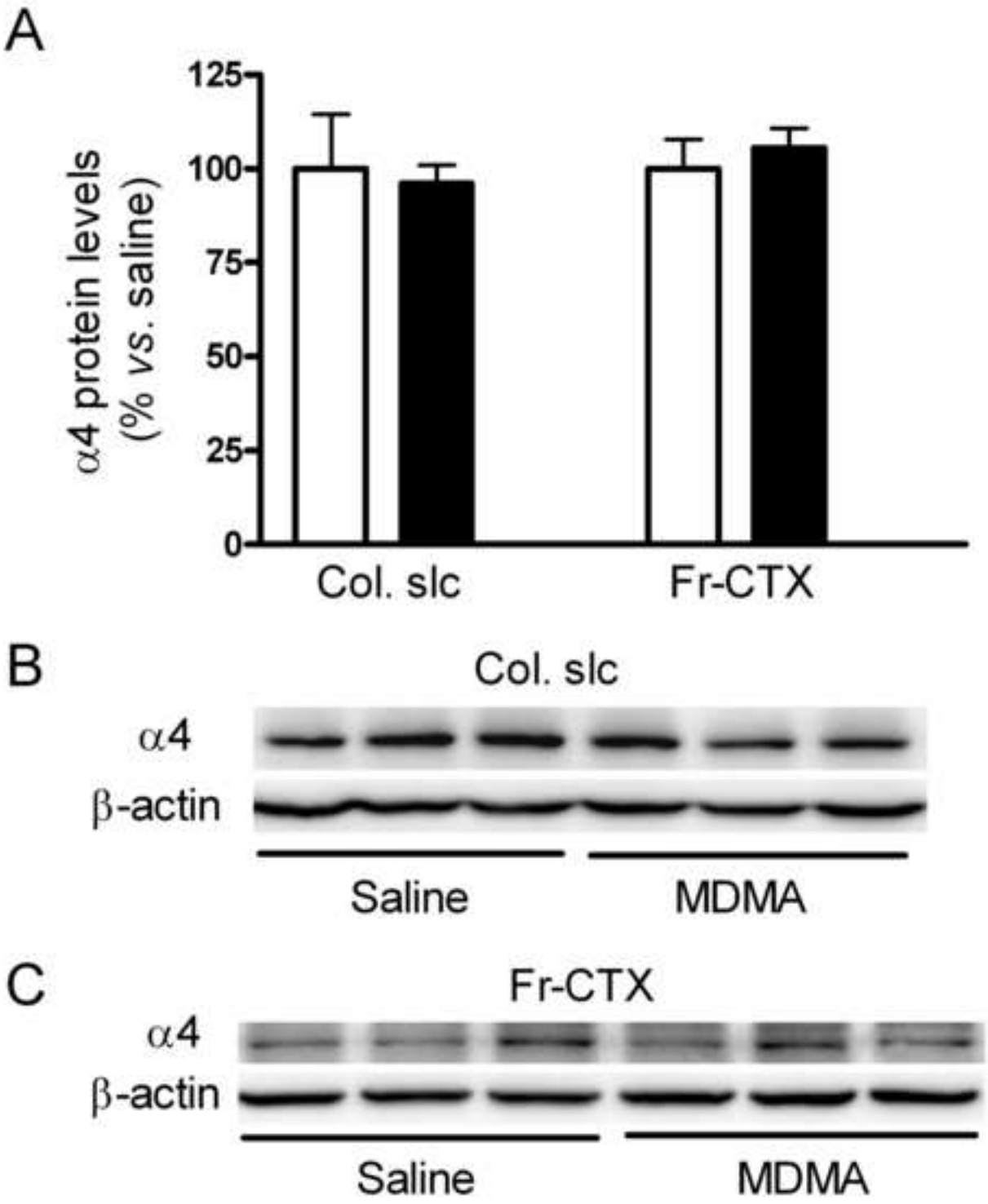

Figure 4

Click here to download high resolution image